Crystalline Sulfur Dioxide: Crystal Field Splittings,

Absolute Band Intensities, and Complex Refractive Indices

Derived from Infrared Spectra

by

R. K. Khanna and Guizhi Zhao

Department of Chemistry and Biochemistry

University of Maryland

College Park, Maryland 20742

and

M. J. Ospina* and J. C. Pearl

Goddard Space Flight Center

Greenbelt, Maryland 20771

*NRC Research Associate

Abstract

The infrared absorption spectra of thin crystalline films of sulfur dioxide at 90 K are reported in the 2700 cm^{-1} - 450 cm^{-1} region. The observed multiplicity of the spectral features in the regions of fundamentals is attributed to factor group splittings of the modes in a biaxial crystal lattice and the naturally present minor ^{34}S, ^{36}S and ^{18}O isotopic species. Complex refractive indices determined by an iterative Kramers-Kronig analysis of the extinction data, and absolute band strengths derived from them, are also reported in this region.

Introduction

Sulfur dioxide has been investigated spectroscopically in exhaustive detail.[1-7] Because of its importance as a pollutant in factory and power plant smoke, and in automobile exhausts, methods have been devised for remote sensing of this molecule.[8,9] These methods are based on the characteristic absorption/emission peaks in the ultraviolet and infrared regions.[7,10]

Such remote sensing methods have been used to identify sulfur dioxide on Jupiter's moon, Io. The characteristic emission at 1360 cm^{-1} recorded by the Voyager IRIS experiment was responsible for the unambiguous identification of this gas in the satellite's atmosphere by Pearl, et al.[11] The 2456.2 cm^{-1} band observed in the reflectance spectrum of Io, recorded by Cruikshank, et al.,[12] has been assigned to sulfur dioxide frost[13] on the satellite's surface. This is corroborated by a relatively broad feature, characteristic of solid material, in the thermal emission spectrum of Io recorded by the Voyager infrared experiment; positioned at 552 cm^{-1}; this band has has been identified with solid SO_2 on the surface.[14]

Laboratory data on the extinction coefficient of the 1360 cm^{-1} band of gaseous sulfur dioxide were utilized by Pearl, et al.[11] to estimate the gas abundance in Io's atmosphere. Corresponding modeling of the surface requires laboratory data on the complex refractive indices of appropriate solid materials in the thermal infrared region. No such data for solid sulfur dioxide are available in the literature, although extensive investigations of the vibrational infrared and Raman spectra of crystalline sulfur dioxide have been published.[1,3,6,7,15,16]

In this report, we present a detailed interpretation of the infrared active modes of crystalline sulfur dioxide, thereby clarifying a number of

inconsistencies in previously reported work. From quantitative
transmission data, the complex refractive indices and the integrated
extinction coefficients of the absorption bands are also obtained.

Experimental

The apparatus and procedure are similar to those described in an
earlier report on crystalline C_2N_2.[17]   Sulfur dioxide obtained from
Matheson (99.5%) was further purified by vacuum distillation to remove the
main impurity, carbon dioxide. Thin films (0.27-2.8 μ thickness) were
deposited on a KRS-5 substrate at 90 K and annealed for 30 minutes. The
thicknesses of the films were calculated from the channel fringes in the
near infrared, using a refractive index of 1.53 (based on that of the
liquid, adjusted by using the Lorentz-Lorenz formula).[18] Quantitative
infrared transmission spectra were recorded on a Perkin Elmer 1800 FTIR
instrument. A spectral resolution of 0.6 cm^{-1} was employed throughout the
measured 2700-450 cm^{-1} spectral range. Characteristic spectra of the thin
film samples are reproduced in figure 1.

Data Analysis

An isolated SO_2 molecule (point group C_{2v}) has three fundamental
vibrational modes. In the gas phase the frequencies and the classification
of these modes are:[5]

$$\nu_1 \ (A_1) \ : \ 1151 \ cm^{-1}$$
$$\nu_2 \ (A_1) \ : \ \ 519 \ cm^{-1}$$
$$\nu_3 \ (B_1) \ : \ 1361 \ cm^{-1}$$

In the solid phase the intermolecular interactions produce significant changes in positions and strength of the bands relative to those in the gas phase. Bands due to the naturally present isotopic species $^{34}SO_2$ (4.4%), $^{34}S^{18}OO$ (0.41%) and $^{36}SO_2$ (0.07%) are also observed in both phases.

The crystal structure of SO_2 is orthorhombic (space group C_{2v}^{17}, Z=2) with the molecules occupying C_2 sites.[19] The correlation diagram (figure 2) shows the expected multiplcity of the molecular modes due to crystal field effects. Thus, for ν_1 and ν_2 modes only one of the two crystal field split components (A_1) is infrared active whereas ν_3 is split into two active components (B_1 and B_2). Because of the biaxial nature of the crystal each infrared active mode is further split into 2 components, TO_1 and TO_2.[20] This is precisely what is observed in the spectra.

Peak frequencies derived from our measurements are listed and compared with earlier results in Table 1. In the regions of fundamentals our observed frequencies are very similar to those reported previously. Earlier works have attempted to explain the infrared bands in terms of the normal modes of SO_2 and it isotopic species. Brooker[15] discussed the Raman spectrum of crystalline sulfur dioxide in terms of Transverse (TO) and Longitudinal (LO) modes but failed to recognize the splitting of the TO components in a biaxial crystal. The assignments proposed here are consistent with the predictions based on the crystal field effects, the expected frequency shifts and relative intensities of the naturally present isotopic species.[4] In the following discussion the spectrum is divided into four regions.

a) $\underline{510 - 540 \ cm^{-1}}$

The strongest bands, centered at 520.9 cm^{-1} and 522.7 cm^{-1}, are assigned to the 2 TO components of the ν_2 (A_1) mode. The two weak

shoulders peaked at 516.7 cm^{-1} and 514.0 cm^{-1} are associated with the ν_2 modes of S^{18}OO and ^{36}SO$_2$ species respectively. The observed shifts of these peaks from the average frequency of the two main TO components (5.1 cm^{-1} for S^{18}OO and 7.8 cm^{-1} for ^{36}SO$_2$) compare favorably with the corresponding calculated values[4] of 4.6 cm^{-1} and 10.6 cm^{-1}.

b) <u>1120 - 1150 cm^{-1}</u>

Results in this region follow from arguments similar to those for the ν_2 region because the ν_1 and ν_2 modes have the same symmetry characters. The two TO components are associated with the 1140.0 cm^{-1} and the 1143.0 cm^{-1} peaks; in all previous work the band at 1140.0 cm^{-1} had been assigned to ν_1 of ^{34}SO$_2$. However, its observed intensity relative to that of the ν_1(SO$_2$) is much larger than the expected 4.4%; in addition, the shift of 3 cm^{-1} from the main peak at 1143.0 cm^{-1} is substantially smaller than the calculated value, 7.3 cm^{-1}. Here we associate the weak shoulder at 1134.0 cm^{-1} with ^{34}SO$_2$; we associate the shoulder at 1120.5 cm^{-1} with S^{18}OO. Both of these assignments are consistent with their relative intensities and the respective calculated frequency shifts[2] 7.3 cm^{-1}, and 28.2 cm^{-1}.

c) <u>1280 - 1350 cm^{-1}</u>

As discussed above, 4 TO components (2B$_1$ and 2B$_2$) of ν_3 are expected in the infrared spectrum. These are, in fact, observed at 1302.8 cm^{-1}, 1304.3 cm^{-1}, 1310.1 cm^{-1}, and 1323.3 cm^{-1}. Their classification into B$_1$ and B$_2$ species as given in the table 1 is somewhat arbitrary in the absence of detailed polarization data. Our results were obtained for thin films of randomly oriented crystals. Brooker carried out polarized Raman studies;[15] however, because of partly oriented crystals and significant polycrystallinity of the sample, there was considerable spillover of modes of other spe-

cies in a scattering geometry designed to obtain modes of a specific symmetry. For example, in the scattering geometry, a(cc)b in which only A_1 modes should appear, the band at 1310.6 cm^{-1} assigned to $v_3(B_1,TO)$ appears strongly. We assign the observed infrared peaks at 1295.6 cm^{-1}, 1291.2 cm^{-1}, and 1287.7 cm^{-1} to v_3 modes of $^{34}SO_2$, $S^{18}OO$ and $^{36}SO_2$, respectively. Their relative intensities are roughly in the ratios of their natural abundance and their frequency shifts from the average of the four main components (~17.5 cm^{-1}, 21.9 cm^{-1} and 25.3 cm^{-1}, respectively) are in agreement with the corresponding calculated values 16.9 cm^{-1}, 21.0 cm^{-1} and 25.4 cm^{-1}.[4]

d) 2270 cm^{-1} - 2460 cm^{-1}

Sharp features at 2287.4 cm^{-1} and 2273.9 cm^{-1} are assigned to the $2v_1$ overtones of SO_2 and $^{34}SO_2$ species, respectively. The features at 2456.2 cm^{-1} and 2433.7 cm^{-1} have proper relative intensities and spectral shifts to be assigned to the $v_1 + v_3$ combinations of SO_2 and $^{34}SO_2$ species. These assignments are in agreement with those of Barbe, et al.[3]

In the regions of all the fundamentals, broad absorptions are observed on the high frequency side of the TO peaks. These are characteristic of strongly polar modes for which the LO-TO splittings are large; the LO modes are made infrared active by anharmonic lattice interactions.[20] In principle, appropriate scattering geometry can be employed to obtain LO frequencies in the Raman spectra of polar crystals. The reported Raman spectra of SO_2,[15] though not obtained for perfectly oriented crystals, give indications of peaks around 1150 cm^{-1}, 530 cm^{-1}, and 1340 cm^{-1} which may be

associated with LO components of ν_1, ν_2 and ν_3, respectively. These frequencies are in approximately the same range as those of the shoulders in our infrared spectra.

The frequencies of the A_2 components of ν_1 and ν_2 are not established; therefore, the magnitude of crystal field splittings of these modes is not known. As mentioned above, the classification of B_1 and B_2 crystal field split components of ν_3 is also somewhat arbitrary because of lack of polarization data. The basis, for our choice of assignments of ν_3 components (Table 1) is the large splitting (B_1-B_2 separation) expected due to dipole-dipole interaction between strongly polar modes. Strong dipolar interactions are also indicated by the fact that the observed LO-TO splittings (~5 cm^{-1} for ν_1 and ν_2 and ~25 cm^{-1} for ν_3) are roughly proportional to their intensities.[20]

Optical Constants and Band Strengths

To properly evaluate integrated strengths of the bands requires knowledge of the wavenumber dependent absorption coefficient. Thin film measurements do not provide this function directly because the transmitted signal is reduced by reflection losses at the sample surfaces, as well as by absorption within the sample. Both of these effects are related to the complex refractive index of the material $m(\nu) = n(\nu) - ik(\nu)$.

To derive $m(\nu)$ from the data, an iterative procedure similar to that suggested by Warren[21] was adopted. Taking account of both reflection and absorption, the intensity transmitted through a plane absorbing film of thickness d deposited on a nonabsorbing substrate is given approximately by[21,22]

$$I_T = \frac{(1-R_1)(1-R_2)(1-R_3)}{1-R_1 R_2} \, e^{-\alpha d}$$

Here

$\alpha \quad = 4\pi \nu k$

R_1 = reflection coefficient at the vacuum-film interface

R_2 = reflection coefficient at the film-substrate interface

R_3 = reflection coefficient at the substrate-vacuum interface

The transmittance, T, is defined as the ratio of the measured intensity to the baseline:

$$T = \frac{I_T}{I_{Baseline}}$$

$$\approx \frac{(1-R_1)(1-R_2)}{1-R_1 - R_2} \cdot \frac{1-R_2^* R_3}{(1-R_1^*)(1-R_2^*)} \, e^{-\alpha_{True} d}$$

where * refers to conditions just outside the regions of absorption bands.

To initiate the iterative procedure, an estimate of the true absorption coefficient, α_{True}, is obtained from the ratio of transmission spectra for two different sample thicknesses (the reflection losses are thereby cancelled, to a first approximation):

$$\alpha_{True} \approx \frac{1}{d_1 - d_2} \ln \left(\frac{T_2}{T_1} \right)$$

The corresponding k values are then used in a Kramers-Kronig analysis to evaluate the real part, n, of the refractive index of the film. A new estimate of α_{True} is then obtained by using the n and k values in the expression

$$\frac{-\ln T}{d} = \alpha_{True} + \frac{1}{d} \ln \frac{(1-R_1^*(1-R_2^*)(1-R_1 R_2)}{(1-R_1)(1-R_2)(1-R_2^* R_3)}$$

Obtaining n through the Kramers-Kronig analysis and reevaluating α_{True} defines the procedure which was iterated to convergence.

In practice, the method was only applied within absorption bands, for in addition to the absorption signatures of SO_2, the actual data contain: a) weak absorption features associated with impurities within the sample and/or the instrument windows (principally H_2O and vacuum pump oil, respectively; these features do not overlap those due to SO_2); b) a slight slope due to instrumental adjustment (this is not caused by scattering in the samples, all of which were clear and transparent to the eye; in addition, the signal decreases with decreasing wavenumber whereas that due to scattering would increase with decreasing wavenumber); and c) channel fringes due to coherent addition of radiation multiply reflected between the parallel surfaces of the films (these typically had periodicities of 10^3 - 10^4 cm^{-1}). For the present analysis, we assume that T = 1 outside of the absorption bands, and define a baseline within the bands by a linear function which is tangent to the channel fringes at the band edges. Plots of n and k are shown in Figure 3. As a check, the complex refractive indices obtained in this way were used to calculate transmission spectra for samples of known thicknesses; Figure 4 shows observed and calculated transmittance in the 1370 - 1270 cm^{-1} region for three different thicknesses. In all cases the agreement with the laboratory data is within 10%. Because of the choice of baseline, the complex refractive indices in the wings of the absorption bands are somewhat distorted. We consider the k values accurate to $\pm$ 10% within the central regions of the fundamentals and to $\pm$ 20% for the weak $2\nu_1$ band. Table 2 gives selected n and k values in the regions of the fundamentals.

The derived absorption coefficients were used to determine the integrated band strengths

$$A = \int \alpha_{True}(\tilde{\nu}) d\tilde{\nu}$$

Results are given in Table 3, along with approximate values derived by a least squares fit to the transmittance data uncorrected for reflection losses:

$$A^* = -\frac{1}{d} \int \ln T(\tilde{\nu}) d\tilde{\nu}$$

Also included in the table are the integrated band strengths for the gas.

The greatest source of error in these determinations is in the thickness measurements of the films. We estimate this error to be $\pm$ 10%. For weaker combination and overtone bands there is an additional error, possibly up to 10% in the measurement of their integrated absorbance areas. Overall we consider our results good to within 10% for the fundamentals and to within 20% for the weaker overtones and combination bands. The strengths of the ν_2 and ν_3 bands are not significantly changed on condensation. However, the changes in the strengths of the ν_1 fundamental and the $2\nu_1$ overtone are substantial, and lie outside the limits of experimental error. The cause of this behavior is unknown, as a clear understanding of the effect of crystal field on the band extinctions is not available at present.

Acknowledgment

References

1. Anderson, A., and Campbell, W. C. W., J. Chem. Phys. 67, 4300 (1977).

2. Maillard, D., Allavena, M., and Perchard, J. P., Adv. Phys. 13, 423 (1975).

3. Barbe, A., Delahaigue, A., and Jouve, P., Spectrochim. Acta. 27A, 1439 (1971).

4. Allavena, M., Rysnik, R., White, D., Calder, V., and Mann, D. E., J. Chem. Phys. 50, 3399 (1969).

5. Giguere, P. A., and Savoie, R., Can J. Chem. 43, 2367 (1965).

6. Anderson, A., and Savoie, R., Can. J. Chem. 43, 2271 (1965).

7. Giguere, P. A., and Falk, M., Can. J. Chem. 34, 1833 (1956).

8. Staehr, W., Lahmann, W., and Weitkamp, C., Appl. Opt. 24, 1950 (1985).

9. Kraisler, O. D., Goldovskii, V. L., Shurenko, Yu. A., and Kozubovskii. Opt. Spectros. (USSR) 51, 320 (1981).

10. Weiner, R. N., and Nixon, E. R., J. Chem. Phys. 25, 175 (1956).

11. Pearl, J., Hanel, R., Kunde, V., Maguire, W., Fox, F., Gupta, S., Ponnamperuma, C., and Rulin, F., Nature 280, 755 (1979).

12. Cruikshank, D. P., Jones, T. J., and Pilcher, C. B., Astrophys. J. 225, L89 (1978).

13. Fanale, F. P., Brown, R. H., Cruikshank, D. P., and Clark, R. N., Nature 280, 761 (1979).

14. Pearl, J., Hanel, R., Ospina, M., Samuelson, R., Jere, G. and Khanna, R. K., IAU Colloq. 77 "Natural Satellites", Ithaca, New York (1983).

15. Brooker, M. H., J. Mol. Struct. 112, 221 (1984).

16. Gerding, H., and Ypenburg, J. W., Recueil, 86, 459 (1967).

17. Ospina, M., Zhao, G., and Khanna, R., Spectrochim. Acta. (1987), in press.

18. Francis, A. W., J. Chem. Eng. Data 5, 534 (1960).

19. Post, B., Schwartz, R. S., and Fankuchen, I., Acta. Cryst. 5, 372 (1952).

20. Decius, J.C. and Hexter, R. M., Molecular Vibrations in Crystals. McGraw Hill Inc. (1977).

21. Warren, S. J., Appl. Opt. 25, 2650 (1986).

22. Sill, G., Fink, U., and Ferraro, J. R., J. Opt. Soc. Am. 70, 724 (1980).

TABLE 1
Vibrational Frequencies for Crystalline Sulfur
Dioxide; Assignments are based on C_{2v}^{17} Space Group

Anderson and Savoie 1965 IR, 77°K cm^{-1}	Giguere and Falk 1956 IR, 98°K cm^{-1}	Barbe et al. 1971 IR, 77°K cm^{-1}	Brooker 1984 Raman, 77°K cm^{-1}	This Work 1986 IR, 90°K cm^{-1}	Assignment
		514.3		514.0	$\nu_2(A_1)[S^{18}OO]$
	517		517.2	516.7	$\nu_2(A_1)[^{34}SO2]$
	521	522	521.9	520.9	$A_1(TO_1)$
				522.7	$A_1(TO_2)$ $\quad \nu_2(SO_2)$
524			524.3		
	528			~530 (broad shoulder)	$\nu_2(LO)$
	535				
542					
1122	1121	1120.6	1120.5	1120.5	$\nu_1(A_1)[S^{18}OO]$
		1134.9	1134.6	1134.0	$\nu_1(A_1)[^{34}SO_2]$
1141	1140	1140.4	1140.5	1140.0	$A_1(TO_1)$
1144	1144	1144.8	1143.8	1143.0	$A_1(TO_2)$ $\quad \nu_1SO_2$
1148			1148.2	~1150 (broad shoulder)	$\nu_1(LO)$
1153					
		1288		1287.7	$\nu_3[^{36}SO_2]$
				1291.2	$\nu_3[S^{18}OO]$
				1295.6	$\nu_3[^{34}SO_2]$
	1303	1302.8		1302.8	$B_1(TO_1)$
1304			1304	1304.3	$B_1(TO_2)$ $\quad \nu_3SO_2$
			1305.0		

TABLE 1 (Continued)
Vibrational Frequencies for Crystalline Sulfur
Dioxide; Assignments are based on C_{2v}^{17} Space Group

Anderson and Savoie 1965 IR, 77°K cm^{-1}	Giguere and Falk 1956 IR, 98°K cm^{-1}	Barbe et al. 1971 IR, 77°K cm^{-1}	Brooker 1984 Raman, 77°K cm^{-1}	This Work 1986 IR, 98°K cm^{-1}	Assignment
1312	1310	1315.2	1310.6	1310.1	$B_2(TO_1)$
1324	1322	1323.2	1323.6	1323.3	$B_2(TO_2)$ — $\nu_3 SO_2$
1341	1334		1337	~1345 (broad shoulder)	$\nu_3(LO)$
1351			1353		
		2274.3		2273.9	$2\nu_1(^{34}SO_2)$
	2287	2288		2287.4	$2\nu_1(SO_2)$
	2432	2433.5		2433.7	$\nu_1+\nu_3(^{34}SO_2)$
	2455	2456.5		2456.2	$\nu_1+\nu_3(SO_2)$

TABLE 2

Selected Values of n and k in the Infrared Absorption
Regions of Crystalline SO_2

$\tilde{\nu}$ (cm^{-1})	n[1]	k
2458.2	1.506*	0.025
2456.2	1.534	0.062*
2454.3	1.559*	0.027
1400.2	1.361	0.021
1375.0	1.299	0.047
1344.7	0.999*	0.317
1334.5	1.043	0.570
1323.4	1.359	1.399*
1316.5	1.650	0.842
1310.2	2.303	1.410*
1305.7	1.799*	0.539
1304.5	2.142	0.921*
1302.1	2.645*	0.370
1210.0	1.597	0.000
1151.2	1.101*	0.311
1150.0	1.110	0.424
1145.5	1.302	0.902
1143.0	2.178	1.737*
1142.5	3.040*	0.737
1140.0	2.138	0.976*
1800.0	1.564	0.00
550.5	1.381	0.023
537.3	1.161*	0.237
522.7	1.772	1.234*
520.9	2.769	1.660*
520.2	3.253*	0.574
516.7	2.066	0.079*

[1] Values of n are based on an assumed value of 1.53 at 2700 cm^{-1} in the Kramers-Kronig analysis of the absorption data.

Data for n and k at 0.3 cm^{-1} interval in the absorption regions are available from the authors.

* Peak positions.

TABLE 3

Integrated Band Strengths for Gaseous and Solid
SO_2 (All Values in Units of 10^4 cm^{-2})

Band	A_{Gas}	A_{Solid}	A_{Solid}^*
ν_1	7.6	13.6	15.2
ν_2	9.4	8.7	12.0
ν_3	67.8	61.8	68.5
$2\nu_1$	0.79	0.16	0.13
$\nu_1+\nu_3$	0.97	1.09	0.97

Figure Captions

Figure 1. Infrared transmission spectra of thin films of crystalline SO_2 at
90 K

(a) 2.8 micron thickness

(b) 0.27 micron thickness

Transmission scales have been arbitrarily shifted for the two

spectra.

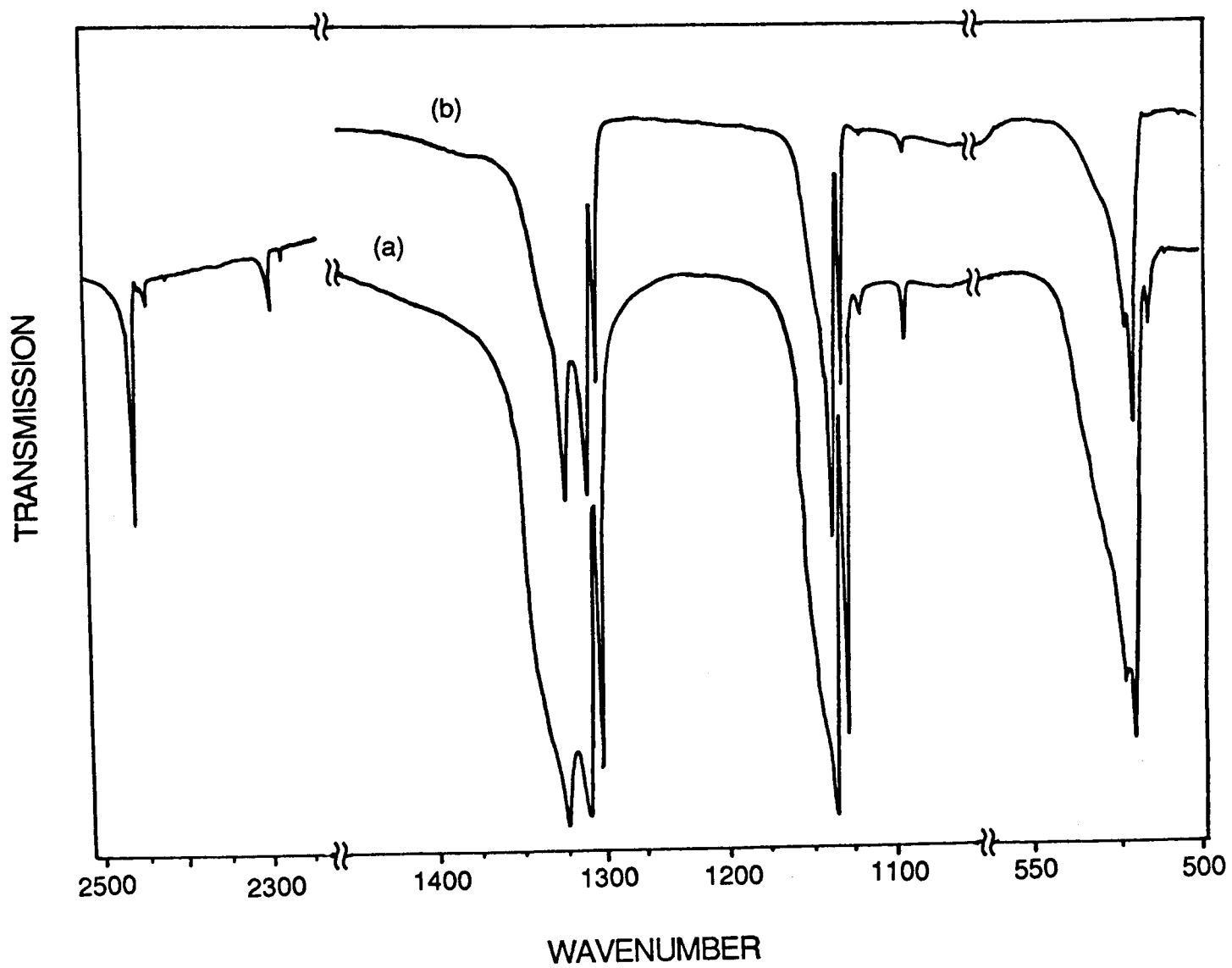Figure 2. Correlation of vibrational modes of SO_2 molecules in crystalline SO_2.

Figure 3. Complex refractive indices of crystalline SO_2 at 90 K.

Figure 4. Comparison of calculated ($\cdots$) and laboratory (——) transmission
spectra in the ν_3 region.

(a) 0.27 μ sample thickness

(b) 0.52 μ sample thickness

(c) 0.75 μ sample thickness

Molecular Group (C_{2v})	Site Group (C_2)	Factor Group (C_{2v})	Selection Rules
ν_1, ν_2 A_1 ———	A	$A_1\ (T_Z)$	IR , R (TO_1, TO_2)
		A_2	-- , R
ν_3 B_1 ———	B	$B_1\ T(\chi)$	IR , R (TO_1, TO_2)
		$B_2\ (T_Y)$	IR , R (TO_1, TO_2)

IR: Infrared Active

R: Raman Active

T_X, T_Y, T_Z indicate directions of dipole change during vibration

TO_1, TO_2: Two possible phonon propagation directions perpendicular to the direction of dipole change